

Published in final edited form as:

*Lab Chip*. 2013 April 21; 13(8): 1468–1471. doi:10.1039/c3lc41362d.

## Rapid fabrication of nickel molds for prototyping embossed plastic microfluidic devices

Richard Novak<sup>a</sup>, Navpreet Ranu<sup>b</sup>, and Richard A. Mathies<sup>\*,a,c</sup>

<sup>a</sup>Program in Bioengineering, UC Berkeley, Berkeley, CA, USA. rnovak@berkeley.edu

<sup>b</sup>Department of Bioengineering, MIT, Cambridge, MA, USA; nranu@mit.edu

<sup>c</sup>Department of Chemistry, UC Berkeley, Berkeley, CA, 94720 USA

### Abstract

The production of hot embossed plastic microfluidic devices is demonstrated in 1–2 h by exploiting vinyl adhesive stickers as masks for electroplating nickel molds. The sticker masks are cut directly from a CAD design using a cutting plotter and transferred to steel wafers for nickel electroplating. The resulting nickel molds are used to hot emboss a variety of plastic substrates, including cyclo-olefin copolymer and THV fluorinated thermoplastic elastomer. Completed devices are formed by bonding a blank sheet to the embossed layer using a solvent-assisted lamination method. For example, a microfluidic valve array or automaton and a droplet generator were fabricated with less than 100  $\mu\text{m}$  x-y plane feature resolution, to within 9% of the target height, and with  $90\pm 11\%$  height uniformity over 5 cm. This approach for mold fabrication, embossing, and bonding reduces fabrication time and cost for research applications by avoiding photoresists, lithography masks, and the cleanroom.

### Introduction

Microfluidic devices have been fabricated from silicon, glass, and poly(dimethyl siloxane) (PDMS), but there is now a move toward thermoset and thermoplastic materials, especially for commercial applications.<sup>1–3</sup> The wide variety of polymers offers a choice of material properties for microfluidics-based sensors and analyzers, including hydrophobicity, flexibility, elasticity, adsorption, and light transmission.<sup>1–5</sup> Furthermore, plastic chips can be integrated with electrodes<sup>6</sup> and surface functionalized<sup>7</sup> like those made from glass and PDMS.

Despite the practical and commercial advantages of plastic microfluidics, plastic materials are not commonly used in research applications. One possible explanation for this disconnect is the lack of simple, inexpensive, and rapid plastic prototyping methods. Hot embossing and injection molding machines for high throughput applications are expensive and not part of most microfabrication facilities. In addition, the fabrication of metal molds used in both systems is time consuming and does not lend itself to rapid prototyping. As a result, significant effort has gone into the development of alternative plastic microfluidics prototyping methods.<sup>8</sup> Milled steel, aluminum, and brass,<sup>2,4,9</sup> cast PDMS,<sup>10,11</sup> epoxy,<sup>12,13</sup> and photoresist<sup>14,15</sup> have all been used as hot embossing molds for low throughput and prototyping applications. However, many of these methods still suffer from relatively long

fabrication times and cannot withstand more than several dozen embossing cycles. Milled metal molds take significant time to fabricate, require high-precision milling machines, and can be relatively limited in resolution. Other plastic fabrication approaches, such as laser engraving,<sup>16</sup> xurography,<sup>17,18</sup> and thermoset polymer casting of SU-8 molds<sup>19,20</sup> offer low production rates and limited materials.

As an alternative, we describe here a “sticker mask” fabrication method that offers rapid and inexpensive prototyping of nickel molds for hot embossing of microfluidic devices within 1–2 h starting from a CAD design. The sticker mask approach is based on cutting vinyl adhesive films with a plotter to generate an insulating mask on a steel wafer. The exposed designs are electroplated to form raised features, which are hot embossed using a hydraulic press with a simple heated platen insert followed by bonding to a featureless plastic sheet. Sticker mask microfabrication offers researchers access to a versatile and simple fabrication process for plastic microfluidic devices.

## Experimental

### Fabrication of nickel molds

A Graphtec Craft Robo Pro CE5000-40 Cutting Plotter (Graphtec America, Inc.) was used to plot CAD designs directly from a .dwg or .dxf file with a programmed step size of 10  $\mu\text{m}$ . An 80  $\mu\text{m}$  thick vinyl adhesive film (3M Scotchcal 220, Gerber Scientific Products, Inc.) was used as the positive electroplating mask. Following plotting, features to be plated up were removed manually using fine-tipped forceps. The plotted design was overlaid with laboratory tape prior to removal from the backing substrate. Feature heights greater than 80  $\mu\text{m}$  were formed by layering one or more vinyl adhesive films over the first prior to cutting. Optimal electroplating uniformity was achieved by the addition of 500  $\mu\text{m}$  wide perimeter boundary features within 500  $\mu\text{m}$  of the designs.

Stainless steel sheets (0.030” thick 304 grade steel with a “mirror-like” finish; #9785K51, McMaster-Carr, Inc.) were machined into circular 90 mm diameter wafers and washed with isopropanol and distilled water. Following a nickel strike of the wafer at 235  $\text{A}\cdot\text{m}^{-2}$  for 2 min at 50–55 °C in a continually-stirred Wood’s Nickel Strike Solution (240  $\text{g}\cdot\text{L}^{-1}$   $\text{NiCl}_2\cdot 6\text{H}_2\text{O}$ , 25% v/v HCl) with an electrolytic nickel anode, the sticker mask was transferred to the steel wafer and the transfer tape or film was removed. The exposed features were electroplated to the desired height in a continually-stirred commercial bright nickel plating solution (#42027, Alfa Aesar, Inc.) at 55 °C. Multi-level features were fabricated by uncovering regions with the tallest features, and later removing the sticker mask from lower height features. For a repeatable and uniform plating rate, the sticker mask-coated wafer and the nickel anode were held in place in a custom acrylic manifold. A laboratory power supply (GPS-3030DD, Instek, Inc.) was used in current control mode to regulate the plating current density. Any remaining adhesive following sticker removal was dissolved with a 1:1 mixture of acetone and toluene. Care should be taken with handling and disposal of nickel salt solutions as nickel contact can cause allergic reactions in some people and ingestion or inhalation has been associated with increased cancer risk.

### Hot embossing plastic microfluidic devices

Zeonor 1060R and 1420R cyclo-olefin copolymer (COC) sheets (1 mm thick) were obtained directly from Zeon Chemical, Inc. Extruded 250  $\mu\text{m}$  thick THV500 samples were kindly provided by Dyneon, Inc. Hot embossing was performed in a hot embossing insert built in-house (see Fig. S1 and design details in ESI) attached to an H6231Z 10 Ton Hydraulic Press (Grizzly Industrial, Inc.). A sheet of polymer was sandwiched between the nickel mold and a sheet of glass and placed between the heated platens. Best results were obtained at pressures

of 5–15 MPa for 0.5–2 min and  $>10$  °C above the polymer's glass transition temperature ( $T_g$ ). Devices were cooled under pressure and de-embossed 10 °C below  $T_g$ .

### Device assembly

Following drilling of via holes, devices were cleaned with distilled water and isopropyl alcohol and dried with nitrogen prior to bonding. Rapid bonding of the embossed COC sheets was accomplished using a solvent-assisted lamination approach modified from the work of Miserere *et al.*<sup>14</sup> We identified *o*-xylene as an optimal solvent for bonding COC devices due to the absence of hazing or cracking, compared to cyclohexane<sup>21</sup> and hexadecane,<sup>14</sup> and low toxicity and carcinogenicity. Specifically, pipetting 1:1 *o*-xylene:isopropyl alcohol to cover the featureless polymer sheet and incubating for 30 s (Zeonor 1420R) or 10 s (Zeonor 1060R) resulted in a thin low- $T_g$  layer that could be laminated to the embossed sheet at temperatures that would not distort the channels. The sheets were quickly dried with nitrogen prior to bonding at or slightly below the polymers'  $T_g$  in a Peach 3500 Photo Pouch Laminator (PEACH 3500, Oregon Laminations, Inc.) at the slowest speed setting. THV500 devices were washed briefly with acetone and dried prior to laminator bonding. Additional experimental details can be found in the ESI.

### Results and Discussion

Nickel hot embossing molds for prototyping plastic microfluidic devices were fabricated using vinyl sticker patterns as shown in the workflow in Figure 1. In Fig. 1A, a cutting plotter translates the CAD design into a sheet of vinyl adhesive, and the cut features are removed. Fig. 1B shows the plotted sticker used as an insulating mask for electroplating a steel wafer. Electroplating the exposed features in a nickel sulfamate bath (Fig. 1C) forms raised structures. Fig. 1D shows hot embossing of the mold into plastic sheets to produce microfluidic devices using a hydraulic press with heated platen inserts as shown in Fig. S1. The embossed features are closed by bonding a sheet of featureless polymer using a solvent-assisted bonding method. The overall time required for producing functional microfluidic devices from digital CAD designs was as low as 1 h. Even the most complex and tall designs tested did not require more than 3 h. A single mold costs approximately \$2 in materials: \$1.50 per steel wafer (not including machining labor), \$0.25 for each of the two vinyl adhesive sheets, and negligible cost for the electroplating chemicals per wafer. This is in contrast to recent polymer device fabrication methods that are either slow and expensive<sup>21</sup> or relatively fast ( $<2$  h starting with a prepared UV mask) but produce relatively weak and deformable molds that are limited to hot embossing only low  $T_g$  materials.<sup>14</sup> The sticker mask approach resulted in durable nickel and steel molds that could be used to emboss devices into a wide range of polymers.

The plotting accuracy, electroplating rates, and feature quality for the sticker mask approach were characterized. Fig. 2A shows the relationship between theoretical feature dimensions in the CAD design and experimental feature dimensions of electroplated nickel molds. The slope of the regression line (1.006) and value of the correlation coefficient (0.999) indicate a high degree of plotting precision and accuracy over the range tested. We observed a real resolution limit of approximately 100  $\mu\text{m}$  as shown by the inability to plot features below 100  $\mu\text{m}$ . This could be due to slight lateral movement of the vinyl sheet during cutting as well as momentum of the blade assembly. The addition of small ( $\sim 5$ –10  $\mu\text{m}$ ) rectangular features before and after any large steps or changes in direction improves the final design resolution when cutting features smaller than 200  $\mu\text{m}$  by reducing blade momentum and minimizing travel distance between reference points. Multi-layer sticker masks only slightly decreased the resolution limit. Since many microfluidic devices consist of relatively wide channels, the 100  $\mu\text{m}$  lateral resolution is not a significant drawback in such devices, and the

tight control of feature height in a relatively rigid polymer is attractive for applications such as imaging-based cell assays<sup>22</sup> or for control of flow-induced shear.<sup>23</sup> For higher resolution features, nickel production molds can be fabricated using SU-8 photolithography with only minimal modifications to the workflow.

Fig. 2B explores the dependence of electroplating rate as a function of current densities. The plating rate is expected to be proportional to the current density based on the following equation:

$$\text{rate} = \frac{60,000 \cdot \varepsilon \cdot I \cdot A}{Q \cdot F \cdot \rho \cdot S}$$

The rate is a function of the efficiency ( $\varepsilon$ ), current ( $I$ , Amperes), molecular mass ( $A$ , g-mol<sup>-1</sup>), charge of the nickel ions ( $Q$ ), Faraday's constant ( $F$ , Coulomb-mol<sup>-1</sup>), nickel density ( $\rho$ , g-cm<sup>-3</sup>), and exposed surface area of the cathode ( $S$ , cm<sup>2</sup>). The 60,000 multiplier is used to convert the electroplating rate to  $\mu\text{m}\cdot\text{min}^{-1}$ . The slope of the data indicates an efficiency of 53% relative to the maximum theoretical plating rate across a wide range of feature sizes and currents tested. It is important to include the exposed wafer edges in the total surface area calculation (2.2 cm<sup>2</sup> for the wafers used here), particularly in the case of small features, to accurately predict the plating rate. We were able to predict the final feature height to within 9% of the actual height and the observed height uniformity was 90±11% across 5 cm.

Reducing the lipping of plated features is important to achieve uniform feature heights. Lipping occurs due to greater electric field density at the edges of a conductive surface where electric field lines concentrate. To minimize this undesirable effect, boundary features were added at constant distances from all perimeter features in the design to improve the current density distribution of exposed cathode surfaces. The addition of boundaries was not necessary for high-density features and did not impede the fabrication of complex designs. Fig. S2 presents the degree of lipping as a function of the current density and distance of the boundary features. The plot shows that decreasing current density decreases lipping for all boundary distances, but features with boundary-feature gaps of 250  $\mu\text{m}$  and 500  $\mu\text{m}$  exhibit a 15% lipping at all current densities tested. SEM images showing improved electroplating quality are presented in Fig. S3. This finding indicates that adding boundary features produces reproducible feature heights and maintains mold quality while enabling fast plating rates. The optimal plating rate was found to be 1.5–3  $\mu\text{m}/\text{min}$ . Nickel molds can also be subjected to chemical mechanical polishing to eliminate lipping.

Fig. 3 presents examples of nickel molding and embossed features fabricated using sticker masks. Fig. 3A shows a droplet generator design with boundaries to produce uniform flow rates. Fig. 3B shows a clean flat channel embossed into COC from the mold in Fig. 3A. The nickel mold and embossed design enabled analysis of dimensional stability after hot embossing. For Zeonor 1060R, we observed dimensional fidelity of 101±1% in the x-y plane and 99±1% in the z-axis with respect to the nickel mold. Fig. 3C shows the cross section of a channel and nearby boundary formed by solvent-assisted lamination of an unfeatured 1420R COC wafer to the embossed design. Note the rectangular geometry of the left channel that indicates minimal channel collapse as a result of bonding. The ability of this method to bond extremely low aspect ratio features (< 1:100) in approximately 50  $\mu\text{m}$  deep devices without channel collapse or distortion is demonstrated by the uniform fluorescence of the bonded design in Fig. S4A. A slight increase in fluorescence can be seen around the channel edges due to lipping as a result of not incorporating boundaries during electroplating.

The sticker mold fabrication method was used to create examples of microfluidic features for fluid handling. Pneumatically actuated valves play a critical role in fluid routing operations, including dilutions, combinations, volume splitting, and pumping.<sup>24,25</sup> The plastic microfluidic automaton in Fig. 3D demonstrates the ability of the sticker fabrication method to produce pneumatic valves in COC. Fig. S4B presents a detailed view of a single four-way valve. Valves remained functional for several weeks of operation in pumping applications. Fig. 3E shows the production of 2 nL droplets of PCR mix in fluorinated oil at a rate of approximately 250 Hz in a droplet generator fabricated from the fluorinated elastomer THV500. Droplet generators are becoming widely adopted for digital PCR and single cell analysis<sup>26–28</sup>; easily fabricated disposable polymer droplet generators can be used to avoid cross contamination of samples and obviate the need for surface coating that degrades with use and can disrupt PCR reactions. Sticker masks result in durable nickel and steel molds that others have shown to last over 1,000 molding cycles<sup>21,29</sup> and allow prototyping with the desired materials.

## Conclusions

We have demonstrated and characterized a versatile approach for fabricating nickel molds for plastic device embossing. The sticker-based method can be used to produce microfluidic devices with 100  $\mu\text{m}$  resolution and tight control of feature height. Boundaries incorporated around features improve the quality of electroplated designs and permit production of functional microfluidic components such as valves and droplet generator nozzles. The simplicity and speed of the sticker mold fabrication method make it well suited for rapid prototyping and the production of disposable plastic microdevices.

## Supplementary Material

Refer to Web version on PubMed Central for supplementary material.

## Acknowledgments

The authors would like to thank Paul Lum and Verena Charwat for helpful discussions. RN was supported by an NSF Graduate Research Fellowship, and NR was supported by a Haas Scholars Program grant. Fabrication was performed at the Biomolecular Nanotechnology Center at UC Berkeley. Work was supported by the trans-NIH Genes, Environment and Health Initiative, Biological Response Indicators of Environmental Systems Center Grant U54 ES016115-01 and by the Mathies Royalty Fund.

## Notes and references

1. Fiorini GS, Chiu DT. *BioTechniques*. 2005; 38:429–446. [PubMed: 15786809]
2. Becker H, Locascio LE. *Talanta*. 2002; 56:267–287. [PubMed: 18968500]
3. Chin CD, Linder V, Sia SK. *Lab Chip*. 2012; 12:2118. [PubMed: 22344520]
4. Leech PW. *J. Micromech. Microeng.* 2009; 19:055008.
5. Toepke MW, Beebe DJ. *Lab Chip*. 2006; 6:1484–1486. [PubMed: 17203151]
6. Illa X, Ordeig O, Snakenborg D, Romano-Rodriguez A, Compton RG, Kutter JP. *Lab Chip*. 2010; 10:1254–1261. [PubMed: 20445877]
7. Gubala V, Le NCH, Gandhiraman RP, Coyle C, Daniels S, Williams DE. *Colloids Surfaces B: Biointerf.* 2010; 81:544–548.
8. Jena RK, Yue CY, Lam YC, Tang PS, Gupta A. *Sens. Act. B: Chem.* 2012; 163:233–241.
9. Hupert ML, Guy WJ, Llopis SD, Shadpour H, Rani S, Nikitopoulos DE, Soper SA. *Microfluid Nanofluid.* 2007; 3:1–11.
10. Wang Y, Balowski J, Phillips C, Phillips R, Sims CE, Allbritton NL. *Lab Chip*. 2011; 11:3089–3097. [PubMed: 21811715]

11. Goral VN, Hsieh Y-C, Petzold ON, Faris RA, Yuen PK. *J. Micromech. Microeng.* 2011; 21:017002.
12. Koerner T, Brown L, Xie R, Oleschuk RD. *Sens. Act. B: Chem.* 2005; 107:632–639.
13. Svoboda M, Schrott W, Slouka Z, Pibyl M, Šnita D. *Microelect. Eng.* 2010; 87:1527–1530.
14. Miserere S, Mottet G, Taniga V, Descroix S, Viovy J-L, Malaquin L. *Lab Chip.* 2012; 12:1849. [PubMed: 22487893]
15. Metwally K, Robert L, Queste S, Gauthier-Manuel B, Khan-Malek C. *Microsyst. Tech.* 2012; 18:199–207.
16. Edwards TL, Harper JC, Polsky R, Lopez DM, Wheeler DR, Allen AC, Brozik SM. *Biomicrofluidics.* 2011; 5 044115–044115–14.
17. Bartholomeusz DA, Boutte RW, Andrade JD. *J. Microelectromech. Syst.* 2005; 14:1364–1374.
18. Sundberg SO, Wittwer CT, Gao C, Gale BK. *Anal. Chem.* 2010; 82:1546–1550. [PubMed: 20085301]
19. Fiorini GS, Jeffries GDM, Lim DSW, Kuyper CL, Chiu DT. *Lab Chip.* 2003; 3:158–163. [PubMed: 15100767]
20. Kim J, deMello AJ, Chang S-I, Hong J, O'Hare D. *Lab Chip.* 2011; 11:4108–4112. [PubMed: 21979428]
21. Mair DA, Rolandi M, Snauko M, Noroski R, Svec F, Fréchet JMJ. *Anal. Chem.* 2007; 79:5097–5102. [PubMed: 17530818]
22. van der Meer AD, Vermeul K, Poot AA, Feijen J, Vermes I. *Am. J. Physiol. Heart. Circ. Physiol.* 2010; 298:H719–H725. [PubMed: 19933413]
23. Lu H, Koo LY, Wang WM, Lauffenburger DA, Griffith LG, Jensen KF. *Anal. Chem.* 2004; 76:5257–5264. [PubMed: 15362881]
24. Jensen EC, Bhat BP, Mathies RA. *Lab Chip.* 2010; 10:685–691. [PubMed: 20221555]
25. Grover WH, Skelley AM, Liu CN, Lagally ET, Mathies RA. *Sens. Act. B: Chem.* 2003; 89:315–323.
26. Novak R, Zeng Y, Shuga J, Venugopalan G, Fletcher DA, Smith MT, Mathies RA. *Angew. Chem. Int. Ed.* 2011; 50:390–395.
27. Zeng Y, Novak R, Shuga J, Smith MT, Mathies RA. *Anal. Chem.* 2010; 82:3183–3190. [PubMed: 20192178]
28. Kumaresan P, Yang CJ, Cronier SA, Blazej RG, Mathies RA. *Anal. Chem.* 2008; 80:3522–3529. [PubMed: 18410131]
29. Mair DA, Geiger E, Pisano AP, Fréchet JMJ, Svec F. *Lab Chip.* 2006; 6:1346. [PubMed: 17102848]

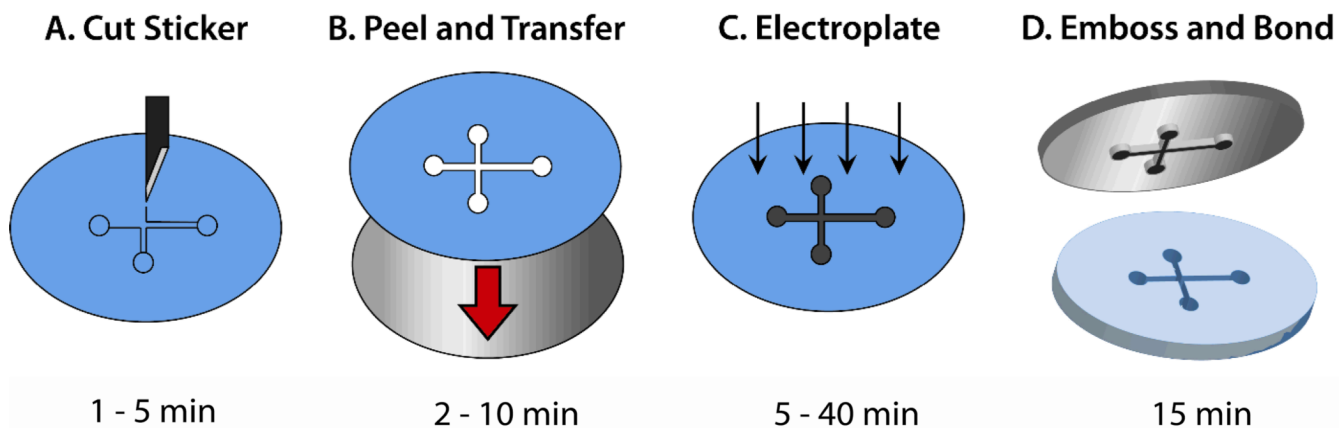


**Figure 1.** Workflow for fabricating hot embossed plastic microfluidic devices. (A) The CAD design is cut into a vinyl sticker using a plotter, (B) transferred to a stainless steel wafer, and (C) electroplated to form the nickel mold. After sticker removal, (D) the nickel mold is hot embossed into the desired plastic. The entire process can take less than 1 h, depending on the complexity of the microfluidic design.

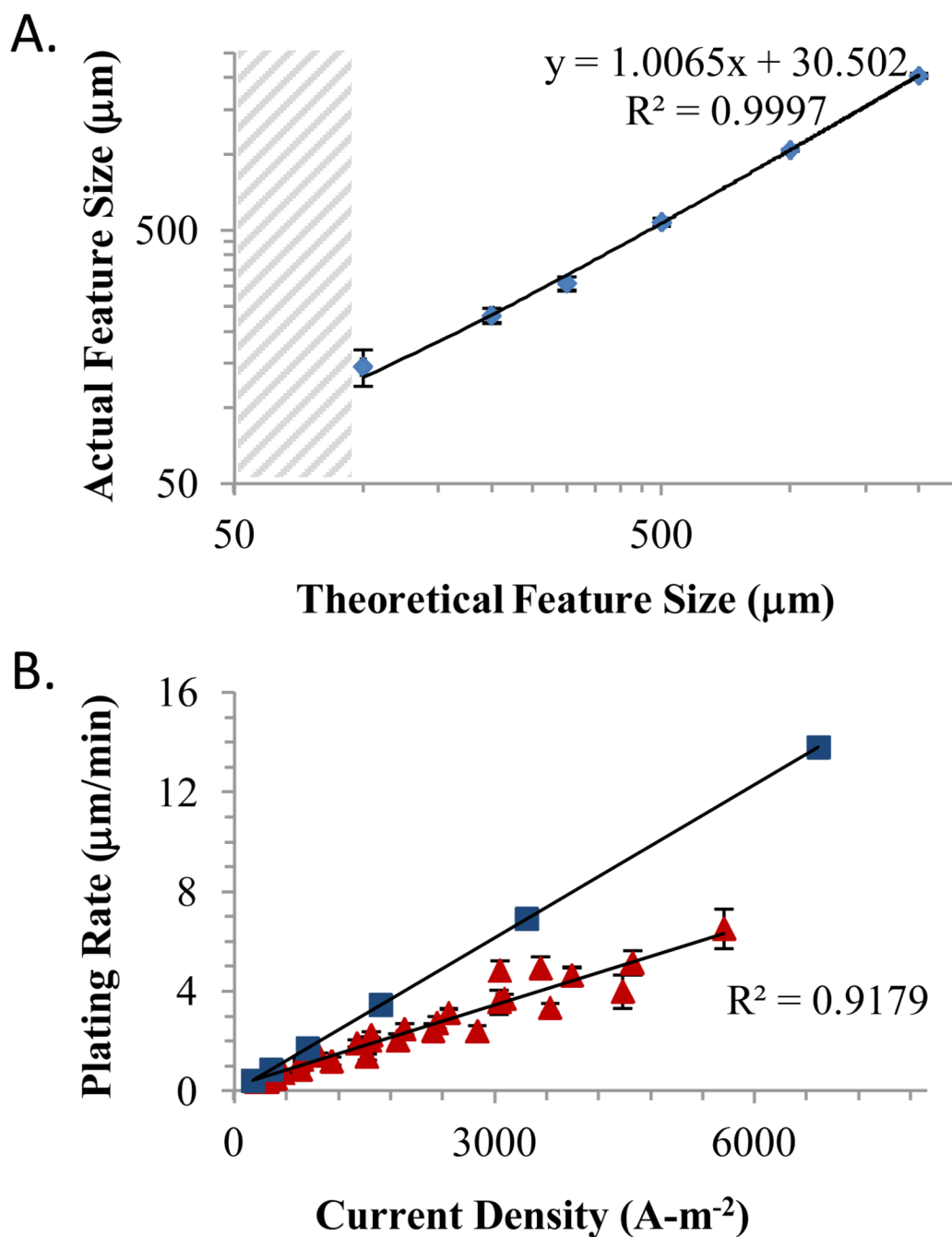


**Figure 2.**

(A) Plot showing a linear correspondence between final nickel feature resolution and the CAD design above  $100\ \mu\text{m}$ ; below  $100\ \mu\text{m}$  the plotter fails to produce distinct features (gray hatching). The resolution is limited by the  $10\ \mu\text{m}$  resolution of the plotter and the stability of the vinyl sticker during cutting. (B) Plot of electroplating rate as a function of current density for a wide range of feature shapes and areas (triangles). The experimental plating efficiency is 53% relative to the theoretical limit (squares). All error bars show standard deviation of the mean.



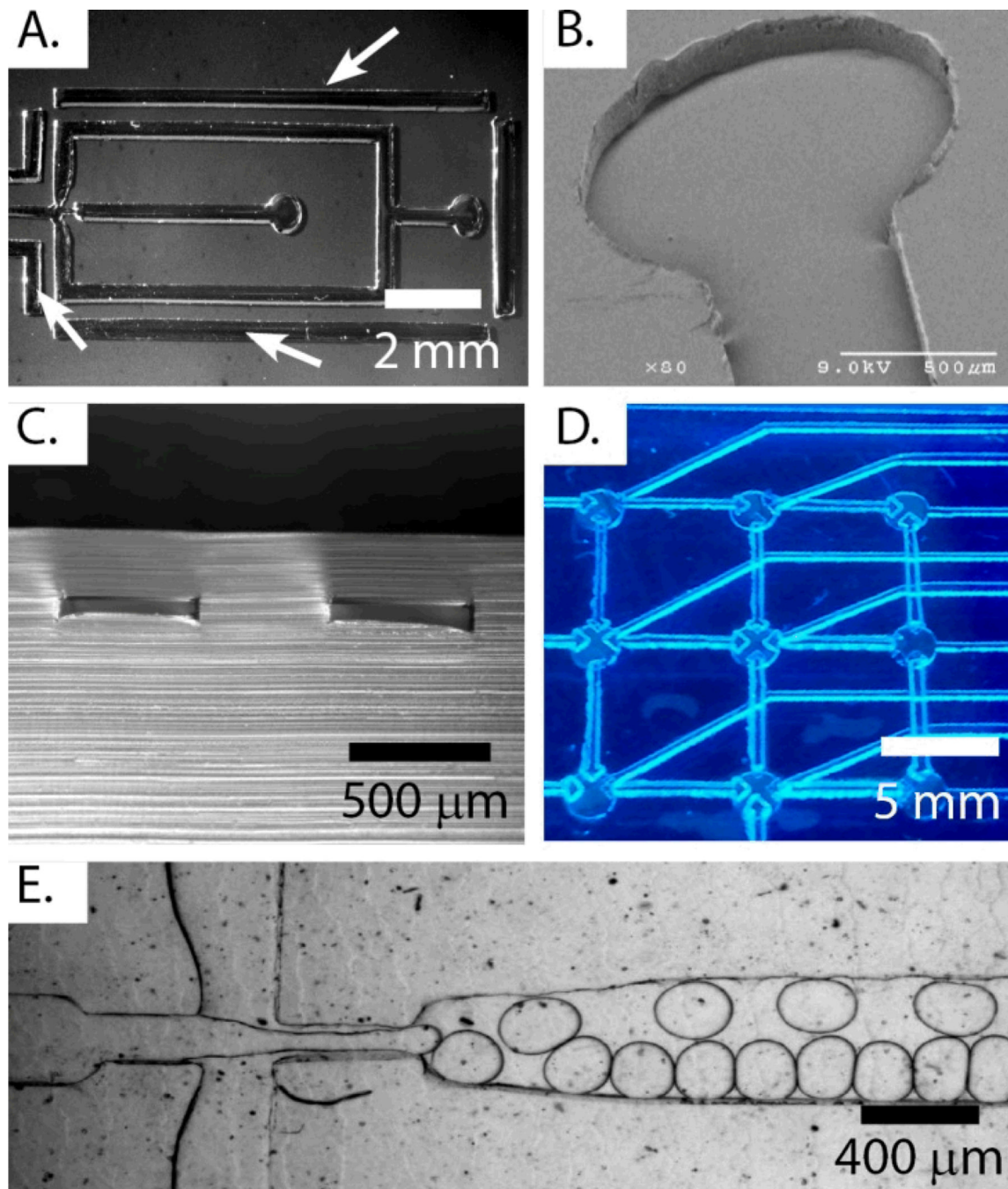


**Figure 3.**

(A) Photograph of nickel mold incorporating electroplating boundaries, indicated by arrows. (B) SEM image of an embossed channel in COC. (C) Xylene-assisted lamination produces low aspect ratio channels in cyclo-olefin copolymer with minimal distortion as seen in this cross section. Note the slight asymmetry of the boundary (right feature) that is used to block stray electrical current to the fluidic channel during electroplating (left). The rapid prototyping method can be used to produce functional components, such as an automaton (D), consisting of an array of pneumatic valves, as well as a droplet generator nozzle (E) made from THV500 fluorinated elastomer.